Electronic structure of polypyrrole films

P. Bätz, D. Schmeisser, and W. Göpel
Institut für Theoretische und Physikalische Chemie, Auf der Morgenstelle 8, Tübingen, Germany
(Received 3 July 1990; revised manuscript received 16 November 1990)

Chemical and electronic properties of polypyrrole films are investigated for different doping levels using x-ray photoelectron spectroscopy (XPS), ultraviolet photoelectron spectroscopy, and high-resolution electron-energy-loss spectroscopy. The XPS results give evidence for instabilities in perchlorate-doped polypyrrole films, whereas tosylate-doped samples are chemically stable. The valence-band structure of the latter is in line with the theoretically expected features of this one-dimensional polymer. Upon doping, we observe occupied states and electronic transitions in the gap. At low dopant concentrations (4%) these states are polaronic. At around 10% doping they cause a semiconductor-metal transition. The finite density of states at the Fermi energy is in accordance with polaronic bands modulated by Coulomb repulsion, as well as with a disorder-induced destabilization of the Peierls ground state.

I. INTRODUCTION

Conducting polymers have been the subject of steadily growing interest in the past 15 years because of their structural and electronic properties,[1] which promised a great number of new applications.[2] Polypyrrole (PPy) is a very interesting candidate for such applications because of its good environmental stability,[3] good mechanical properties,[4] high conductivity,[5] and easy preparation.[6] An interesting property of this polymer is the unusual electronic structure, especially the appearance of polarons and bipolarons resulting from particular electron-phonon coupling.[7] PPy is generally considered to belong to the class of one-dimensional polymers having a polyene backbone. This classification is supported by the electrical and chemical behavior of different substituted pyrrole units of various lengths.[8] Regarding PPy as a one-dimensional chain with equidistant carbon positions, a metallic behavior would be expected. In this hypothetic case the electronic structure would be dominated by the uppermost π band which is delocalized along the chain with a dispersion of about 10 eV.[9] This, however, is overcome by the stabilization of the chain in the dimerized form. Due to the dimerization and the symmetry breaking, caused by the presence of the nitrogen atom, the uppermost π band is backfolded and a gap of about 3 eV is opened.[10] This system has electron-phonon-coupled excited states which are believed to be polaronic. This type of electronic structure is representative for a one-dimensional polymer with a nondegenerate ground state. Therefore, PPy is a good candidate to study systematically the influence of doping to the intrinsic defect generation and dynamics in one-dimensional organic conductors.

PPy was examined in recent years by several different spectroscopical techniques with the aim to understand the chemical and electronic structure of this polymer. In spite of considerable effort, there is still some uncertainty about these topics. However, a certain degree of agreement seems to be achieved on some points: PPy is a one-dimensional conductor whose conductivity reaches values up to 10^3 S/cm for heavily doped samples;[11] intrinsic defect states can be generated by doping; these states can be described as nonlinear excitations like polarons or bipolarons, predicted by several theoretical calculations;[12–15] optical[16,17] and high-energy electron-energy-loss[18] (EELS) investigations exhibit low-lying electronic transitions in the band gap, which grow stronger with increasing doping level; electron-paramagnetic-resonance (EPR) measurements[19,20] show a decrease in the number of free spins per injected charge at high doping levels, which could be explained in a bipolaronic model of the conduction mechanism; measurements of the temperature dependence of both conductivity and thermopower[21] indicate PPy to be a *p*-type semiconductor; a three-dimensional variable-range-hopping model can be applied; conductivity measurements have been carried out as a function of various parameters,[11,22] i.e., doping level, temperature, pressure, stretch ratio, type of dopant, preparation conditions, etc.; several photoelectron spectroscopy investigations of PPy (Refs. 23–27) exist up to now; the results differ significantly and depend on the preparation conditions; especially the shoulders observed in the N 1*s* core-level emission structure have been the subject of various explanations.

In the present study we therefore prepared well-defined PPy films with the aim to clarify the above-mentioned questions in detail. We used ultraviolet photoelectron spectroscopy (UPS), x-ray photoelectron spectroscopy (XPS), and high-resolution electron-energy-loss spectroscopy (HREELS) to determine the electronic structure of PPy in the core and valence-band range. These techniques can be used to determine the ionization potential (I_p), the band gap (E_g), and the bandwidth. Their values will serve to discuss the electronic structure of the conducting polymer. The ionization potential indicates whether a given acceptor is capable of ionizing, at least partly, the polymer chains. The band-gap value deter-

mines the intrinsic electronic properties of the material. The difference to the ionization potential gives the electron affinity. The bandwidth of the highest occupied band serves as a measure of the delocalization along the chains and thus may be correlated with the mobility of possible charge carriers in the band. Applying ultrahigh vacuum (UHV) compatible preparation conditions, we have been able to investigate the bulk electronic structure of tosylate (Ts^-)-doped polypyrrole (PPyTs) with the surface sensitive techniques UPS and HREELS.

II. EXPERIMENT

Preparation of PPy films was carried out in a glovebox in N_2 atmosphere [$p(O_2) < 1$ ppm, $p(H_2O) < 300$ ppb]. The films were transferred to the UHV systems[28] in a UHV transfer box. Any contact of the films to air was avoided.[29,30]

PPy films were electrochemically synthesized from a solution of acetonitrile (99.8% Merck) containing 0.06 m pyrrole (Py) and 0.1 m of different electrolytes. Pyrrole was distilled in N_2 atmosphere before using; the other substances were used without further purification. The polymerization takes place in a one-compartment cell containing two platinum sheet electrodes and a Ag/AgCl reference electrode (Metrohm EA440) in ethanol saturated with LiCl with TsH in acetonitrile as intermediate electrolyte. The cell was under potentiostatic control. The cell potential was increased linearly with time from zero to its final value, the scan rate varying between 2 and 10 mV/s. Typical values for the polymerization parameters were $U=0.6$ V, $I=0.2$ mA/cm^2, and $t=5$ min. The amount of water in the polymerization solution was varied between 0.1% and 5%. Reduced films were obtained from a solution of acetonitrile containing 0.1 m of the same electrolyte as used for the polymerization. Typical parameters for the reduction were $U=-0.5$ V, $I=0.04$ mA/cm^2, and $t=2$ h. The electrolytes used were tosylate ($CH_3C_6H_4SO_3H$) and the perchlorates: $NaClO_4$, $AgClO_4$, and Bu_4NClO_4. The molecular structure of tosylate and polypyrrole is shown in Fig. 1. Depending on their thickness, the polymerized films appear black or dark blue. Upon reduction, the color changed to light blue or green. Completely reduced films appear bronze and are almost transparent. For the most important results of these studies we have used five typical dopant concentrations Y: $<1\%$, 4%, 15%, 30%, 40%. The dopant concentrations were determined from the measured charge flow during the sample preparation, according to the electrochemical parameters of similar studies.[22,31,32] The relative XPS intensities gave an independent control of the estimated doping level.

XPS measurements were performed using a VSW instrument, employing Mg $K\alpha$ (1253.6 eV) and Zr $M\zeta$ radiation (151.4 eV). For the UPS measurements He I and He II radiation was used. Calibration of the spectra was done with the core-level structures and the Fermi edge of Au or Pt samples. In the following the binding energy is always referred to the Fermi level (E_F). For the Zr M_ζ radiation the indium 4d core level was used additionally for calibration. The HREELS investigations were carried out at excitation energies from 5 to 200 eV in specular reflection geometry. The full width at half maximum (FWHM) of the elastic peak varied between 10 and 50 meV dependent on the pass energy chosen. The angle of incidence of the electron beam was varied by rotating the probe. The exit angle was varied by swiveling the analyzer. *In situ* XPS, UPS, and HREELS measurements were done in a Leybold spectrometer. The pressure during the measurements was in the 10^{-10} mbar range.

III. RESULTS

The XPS spectra of two typical PPy films are displayed in Fig. 2. The energy ranges around the O 1s, N 1s, C 1s, Cl 2p, and S 2p levels are shown for both Ts^- and ClO_4^- doped films, respectively. The ClO_4^--doped films ($PPyClO_4$) revealed several peculiarities as the intensity ratios for the C 1s and N 1s signals are found to change slightly with time and with doping. The ratios of the O 1s and Cl 2p signals showed strong variations with time

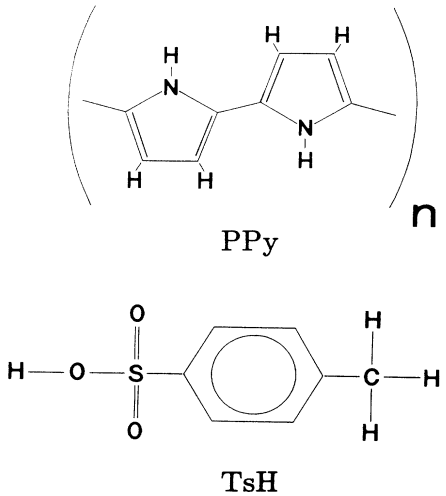

FIG. 1. Molecular structure of polypyrrole and tosylate.

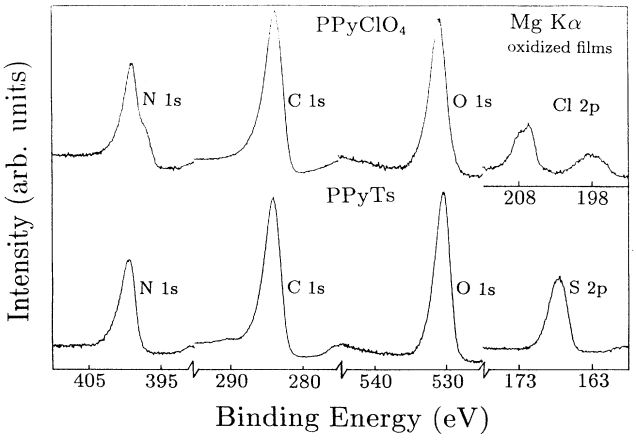

FIG. 2. XPS spectra of the four main structures of PPy films. The different peaks are normalized to almost the same height.

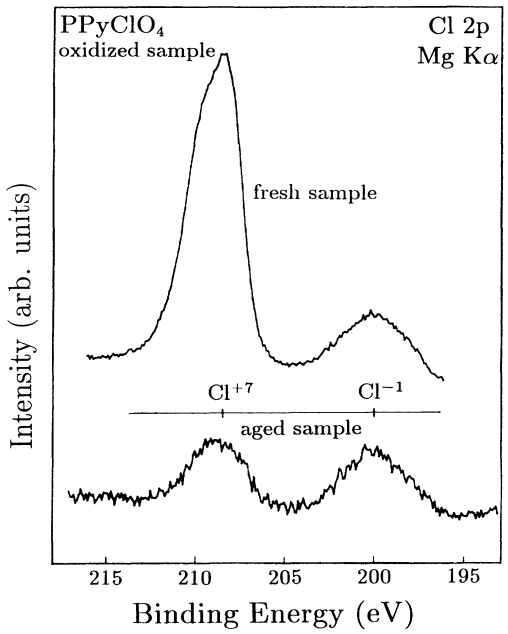

FIG. 3. Cl $2p$ core-level XPS spectra of a freshly produced $PPyClO_4$ film, and of the same sample after five months' storage in air.

and were not reproducible for similarly prepared films. These variations are in line with the simultaneous observation of different chemical species in the Cl $2p$ signal. Besides the expected Cl $2p$ peak at 208 eV (Cl $2p^{+7}$) corresponding to the Cl in the ClO_4^- ion with oxidation state +7, all films show an additional Cl $2p$ structure at 200 eV (Cl $2p^{-1}$) corresponding to the oxidation state −1. The variation of the relative intensities of these signals upon aging, i.e., storage in laboratory atmosphere, is shown in Fig. 3. The same effect was observed less pronounced after storage for two weeks in UHV. Samples investigated under the same conditions before and after aging showed a constant N $1s$/Cl $2p^{-1}$ ratio. Using electrolytes with different cations, thereby varying from the reactive sodium to the noble silver, and further on to the large organic tetrabuthylammonium, does not cause an improved stability in the XPS intensities. In contrast to the ClO_4^--doped films, the Ts^--doped PPy films showed a stable C $1s$/N $1s$ ratio of 7.6. The effect of aging was less pronounced than in ClO_4^--doped samples. The FWHM of the core-level peaks is smaller in PPyTs—the C $1s$ FWHM, in particular, was reduced by 0.6 eV, when compared to that in $PPyClO_4$. The N $1s$ core levels for PPy films with different dopants are shown in Fig. 4(a). Again, they are in general sharper for PPyTs. The ClO_4^--doped films exhibit shoulders at both sides of the N $1s$ peak [top curves in Fig. 4(a)], which could not be correlated with the doping concentration. For Ts^--doped films, on the other hand, the FWHM of 1.7 eV is observed reproducibly and is not affected by the degree of doping. In Fig. 4(b) we have displayed the N $1s$ levels for PPyTs films at $Y \approx 2\%$ (upper curve) and at $Y \approx 30\%$ (lower curve) as typical examples. Another remarkable difference between Ts^-- and ClO_4^--doped films is the occurrence of shake-up satellites at the C $1s$ core-level peak only for PPyTs films. Such satellites, which are an indication of extended π systems, were observed 6.4 eV above the main peak.

The doping concentration can be determined quantitatively from XPS intensities. For ClO_4^- dopants, the ratio of the Cl $2p$ to N $1s$ intensities provides a convenient

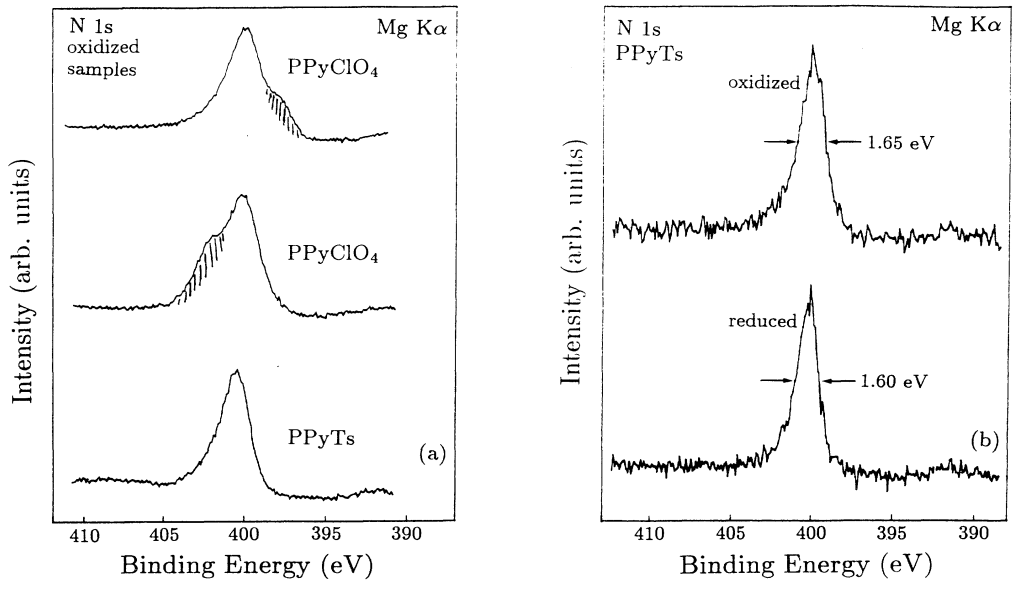

FIG. 4. N $1s$ core-level XPS spectra of (a) differently prepared $PPyClO_4$ films and a typical PPyTs film and (b) PPyTs films in different oxidation states recorded with 10 eV pass energy.

measure of the dopant concentration.[23,24] However, for Ts^- doping, the S 2p intensity with respect to that of the N 1s level determines the amount of dopant molecules, but is not correlated linearly with the number of charge transferred. This is shown in Fig. 5, where the ratio of the peak areas of the N 1s and S 2p XPS structures is plotted against the current density during polymerization. In the range between $I=0.2$ mA/cm^2 and $I=2.5$ mA/cm^2, the N 1s/S 2p ratio is independent of the oxidation state.

The electronic structure of PPyTs is determined from UPS and HREELS. For $PPyClO_4$ the valence-band features are found to be not reproducible and are therefore not shown. In the following we concentrate on the Ts^--doped films. In Fig. 6 we have displayed the He II excited valence-band spectra at different doping levels. We find that the general shape of the spectra is highly reproducible and does not depend on the amount of doping. However, the valence-band features appear sharper at high doping levels. The valence-band range of PPy films is determined from the high-lying π bands, as is evident from the different photoionization cross sections for the various excitation energies used in Fig. 7. We notice that the σ-derived bands appear with higher excitation energies whereas at low photon energies (He I and He II) the valence-band structure is determined from the C 2p- and N 2p-derived π bands. UPS spectra of PPyTs films that were taken after exposure to air of the films show completely different structures. We observe a complete loss of the fine structure; instead, a very broad structure around 9 eV is observed, which is typical for hydrocarbons. These contaminations could be removed by thermal treatment under UHV.

In order to concentrate on the most prominent features of the UPS data, we show in Fig. 8 the He I valence-band spectra of PPy films at different doping levels—in particular, the range around the valence-band maximum (VBM). For the reduced film ($Y<1\%$) the VBM is about 1.2 eV below E_F. In agreement with theory,[9] the density of states (DOS) at the valence-band edge of the upper π band (π_1) is small, as this band has a large width (3 eV) and is derived from the p_z-derived C 2p levels only. Slight doping ($Y\approx4\%$) causes a shift of E_F towards the VBM of about 0.5 eV, indicative of p-type conductivity. This reduction of (E_F-E_V) is not only observable at the VBM. It appears at all XPS and UPS structures as a

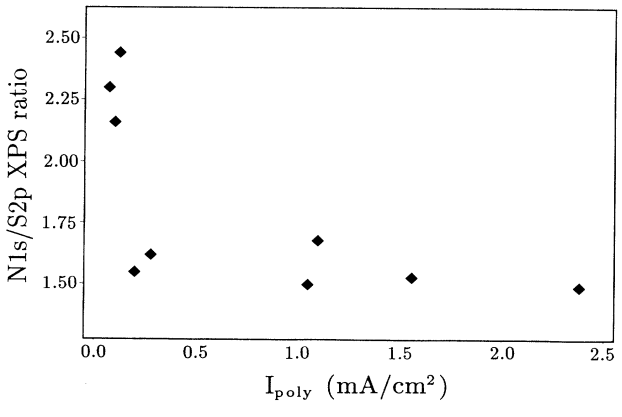

FIG. 5. Ratio of the peak areas of the N 1s and S 2p structures in the XPS spectra of several PPyTs films plotted against the current density during the polymerization of the films.

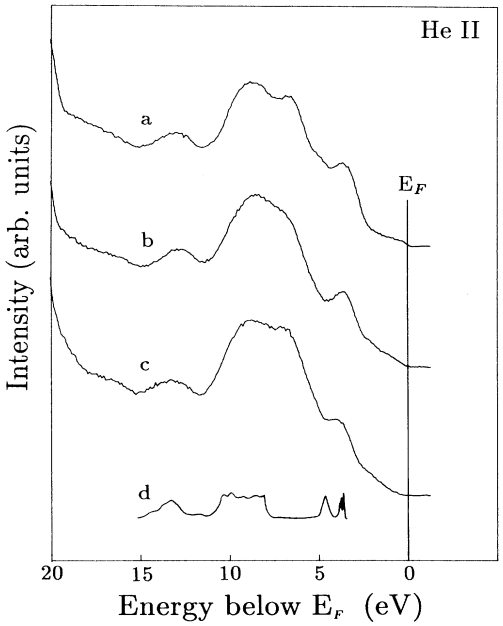

FIG. 6. He II spectra of PPyTs films with dopant concentrations of (a) $Y\approx40\%$, (b) $Y\approx15\%$, and (c) $Y\approx4\%$. For the sake of band assignments, a gas-phase pyrrole spectrum (d) is also shown (Ref. 37).

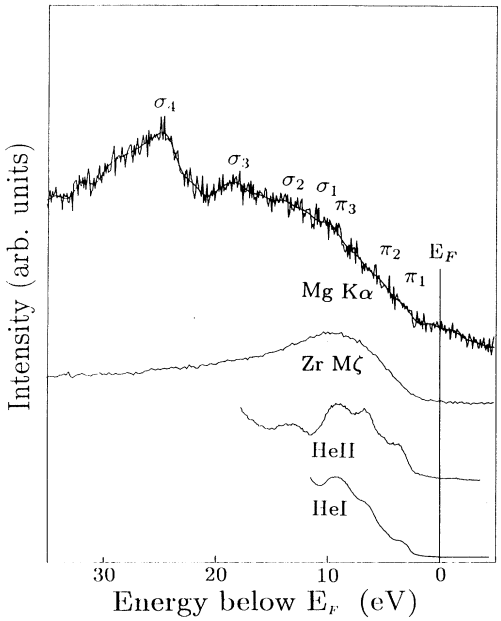

FIG. 7. Valence-band spectra of an oxidized PPyTs film recorded at four different excitation energies. The band assignment is according to Ref. 14.

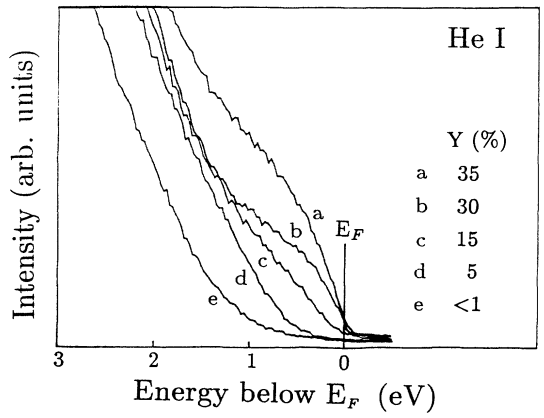

FIG. 8. He I valence-band spectra of the extended range near the valence-band maximum E_V of PPyTs films at different doping levels Y.

shift of the peak position relative to E_F and is also seen at the secondary electron onset (SEO) in the photoemission spectra. After this initial shift at low dopant concentration, the value of $(E_F - E_V)$ remains constant over a wide doping range up to strong oxidized films, i.e., E_F is pinned in the gap. With increasing oxidation rate ($Y \approx 15\%$) we also observe states in the gap, leading to a continuous DOS up to E_F, which is increasing until the emission from the VBM is no longer distinguishable. To demonstrate these changes, we show in Fig. 9 difference spectra obtained from the He I spectra displayed in Fig. 8 indicating the remarkable increase of the DOS in the gap with rising dopant concentration.

Upon doping, changes appear also in the HREELS data as shown in Fig. 10. For almost completely reduced samples ($Y < 1\%$) no electronic losses in the range from 0.5 to 5 eV loss energy are detectable. With increasing dopant concentration ($Y \approx 2\%$), a broad loss structure around 2.4 eV appears. It is composed of two losses at 2.0 and 2.5 eV,[33] the latter being about four times more

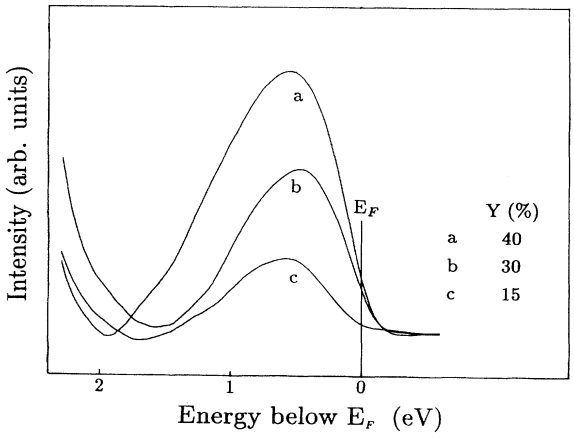

FIG. 9. Difference spectra obtained from the He I spectra shown in Fig. 8.

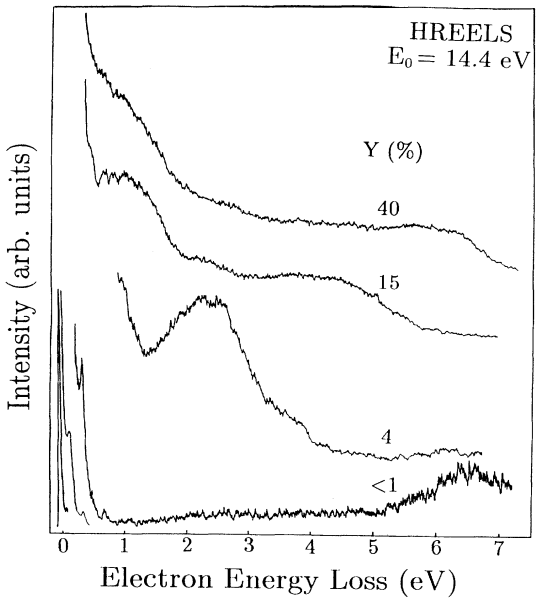

FIG. 10. Electron-energy-loss spectra of PPyTs films at different doping levels Y, recorded with a primary energy $E_0 = 14.4$ eV.

intense. At intermediate doping levels ($Y \approx 15\%$) the most prominent structure is a broad loss peak around 1.1 eV. At higher doping levels ($Y \approx 30\%$) all the loss features almost vanish and a continuous loss spectrum is obtained.

In specular geometry we observe a broad loss feature around 4 eV for intermediate ($Y \approx 15\%$) and high dopant concentrations ($Y \approx 30\%$), which can be assigned to the lowest π-π^* transition that is expected between 3 and 4 eV loss energies.[10] At low doping levels the π-π^* transition is not seen in specular geometry, but appears on changing the angle of detection by swiveling the analyzer out of specular geometry. Figure 11 shows HREEL spectra of a PPy film at low doping level ($Y \approx 4\%$) recorded at different angles of detection. We observed that the broad loss structure around 4 eV is composed of two loss peaks at 3.8 and 4.6 eV, which interfere with the loss structure at 2.4 eV. For this reason, the loss maximum appears at the relatively high value of 3.8 eV (compared to the absorption maximum at 3.2 eV in optical spectra[16]). However, the onset of the loss feature at 3.8 eV is around 2.4 eV, a value which is in excellent agreement with optical[16,17] and high-energy electron-energy-loss spectroscopy (EELS) data.[18] The momentum transfer parallel to the surface ($\Delta k_\parallel$) of electrons with a loss energy ΔE is

$$\Delta k_\parallel = \pi(8m)^{1/2} h^{-1} [E_0^{1/2} \sin\alpha - (E_0 - \Delta E)^{1/2} \sin(\alpha + \theta)] \quad (1)$$

and can be varied by changing the angle of detection. E_0 is the excitation energy, ΔE is the loss energy, and α and θ are the angle of incidence and the angle between exit angle and specular geometry. The calculated values of $\Delta k_\parallel$ are indicated in Fig. 11. The observed losses at 2.4, 3.8, and 4.6 eV show a maximum of their relative intensities when the momentum transfer $\Delta k_\parallel$ is a minimum.

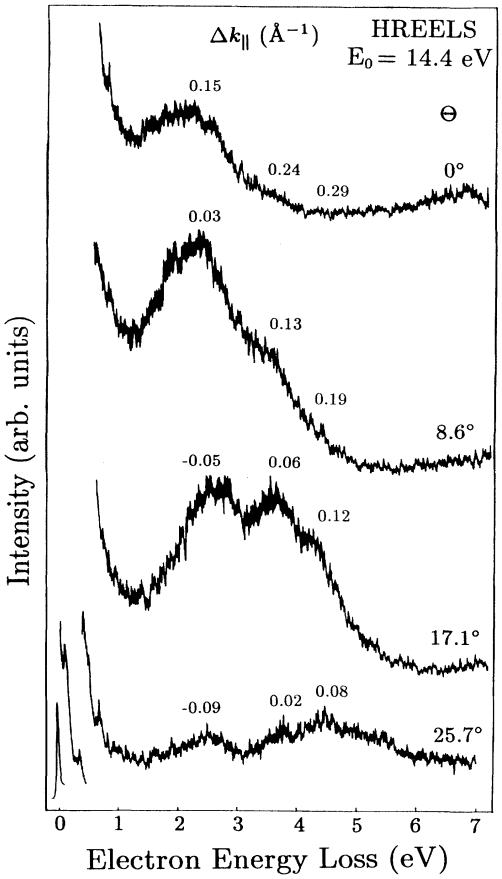

FIG. 11. Electron-energy-loss spectra of a reduced PPyTs film ($Y \approx 4\%$) at different exit angles. θ denotes the angle between the exit angle and specular geometry. The calculated momentum transfer $\Delta k_{\parallel}$ is given for the loss energies 2.4, 3.8, and 4.6 eV.

With increasing dopant concentration, the angular dependence of the spectra decreases and disappears for fully oxidized films. It should be noted that the angular dependence of the loss structures in the HREEL spectra depends on the history of the investigated samples. Samples investigated by HREELS before and after running photoelectron spectra show that the angular dependence of the HREEL spectra decreases considerably if photoelectron spectroscopy investigations were carried out prior to the HREELS measurements. For instance, the loss structure around 4 eV, which is due to the lowest π-π^* transition, is observable at specular geometry for reduced and slightly oxidized samples only after investigation of the samples with photoelectron spectroscopy. We believe that this effect is caused by structural changes in the polymer which occur during the UV and x-ray irradiation in the course of the photoelectron spectroscopy experiments.

IV. DISCUSSION

The electronic structure and its influence on the conductivity mechanism leading to the high conductivity of doped PPy films is the main topic of the following discussion. The electronic structure of organic polymers is mostly treated within a one-dimensional band model because of the high degree of order along the polymer chain and the strong delocalization of the upper π orbital (π_1). Calculations carried out within this model on PPy chains yield a complete band structure.[9,13] The latter exhibits three bonding π bands (π_1, π_2, π_3); two of them are relatively flat (π_2, π_3) and can be assigned to the pyrrole backbone. The remaining upper π band (π_1) shows a strong dispersion of about 3 eV and is assigned to delocalized π electrons, which are responsible for the aromatic character of PPy. The calculations indicate the appearance of two additional bands in the band gap upon doping, which emerge from polaronic or bipolaronic defects on the polymer chain. At high doping levels these intragap bands are expected to broaden until they merge with the valence band and, respectively, the conduction band. A drastic reduction of the band gap is expected. Optical[16,17] and EELS (Ref. 18) investigations support this concept, as they exhibit intragap transitions which are in reasonable agreement with calculated intragap states arising from polarons or bipolarons and which gain intensity with increasing doping level. Especially at high doping levels, results from both methods show a broad structure around 1 eV, which in general is assigned to the transition from the valence band into the lower bipolaron band.

Before discussing our results within this concept, we will discuss the stability of PPy films depending on the counterions used, the electronic structure of the undoped films, and the changes that occur in the electronic structure upon doping.

A. Chemical stability of PPy

In our XPS data, the occurrence of a Cl^- peak (Fig. 3) implies a decomposition of the ClO_4^- ion. The width of the C 1s structure in ClO_4^--doped films and the good stability of the Cl^- signal gives evidence of a chemical bonding of Cl^- to the pyrrole ring in α position. Assuming that this bonding occurs also during the polymerization, a shortening of the chain length would result, which is in agreement with the lack of C 1s shake-up satellites in $PPyClO_4$ films. The observed instabilities in the N 1s, C 1s, and Cl 2p core levels should reflect in the macroscopic properties also. Indeed, the observed instability of ClO_4^--doped films is in agreement with earlier results, which showed a relatively strong decrease of conductivity upon aging[34] and upon heating in an inert atmosphere[3] for PPy films doped with ClO_4^- or other inorganic anions. Ts^--doped films showed a clearly improved stability of the conductivity under the same conditions. The thermal stability of ClO_4^--doped films is also less if compared with that of Ts^--doped films.[35]

The fine structure of the N 1s core level—in particular, the emerging of shoulders on both sides of the peak on increased or reduced doping—has been stressed in former XPS studies.[17,23–25] These studies yield quite different results. The shoulders at the N 1s peak, in particular, appeared at different doping levels. Therefore, no satisfactory explanation for the appearance of these

shoulders has been given up to now. From our results we conclude that the shoulders do not reflect a specific charge distribution within the lateral extension of the defects. Further, their appearance is not connected to the oxidation state of the film. The shoulders rather result from a partial decomposition of the counterion within the films or from exposure of the films to air. This explanation is satisfactory for all XPS investigations on PPy to our knowledge. Former studies reporting on an increase of the shoulders with air exposure of the samples do confirm our explanation. In our opinion, the shoulder at the N 1*s* peak on the low-binding-energy side is caused by deprotonation of the N atom, as suggested before,[16] whereas the shoulders on the high-binding-energy side originate from an exchange of the proton bound to the N atom with OH groups of atomic oxygen. Therefore, we conclude that the appearance of a single sharp N 1*s* structure in photoelectron spectra is characteristic for stoichiometric films as well as for the absence of chemical reactions on the N site within the polymer.

XPS can also be used to determine the dopant mechanism in the films. The intensity of the S 2*p* signal relative to the N 1*s* signal is a direct measure of the amount of tosylate molecules (TsH) and tosylate ions (Ts^-) per monomer unit in the chain. An independent method is to determine the doping level from the current density during the electrochemical preparation of the film. The direct comparison of both methods, as displayed in Fig. 5, allows one to comment on the doping and dedoping mechanism of PPyTs. We expected to find an almost linear variation of the XPS ratio with the polymerization current density. However, as shown in Fig. 5, the relation is strongly nonlinear, indicating that TsH molecules are not completely reduced on polymerization. Rather, a maximum amount of TsH uptake exists, which is reached at very low polymerization current densities around 0.1 mA/cm^2. The complete oxidation of the polymer chains is not expected until a current density of 1 mA/cm is reached.[32] The occurrence of only a small decrease of the N 1*s*/S 2*p* ratio on reduction of the films indicates that only a few Ts^- molecules are removed from the film on reduction. The observed tosylate remaining in the PPyTs films on electrochemical dedoping is assigned to the small mobility of the Ts^- ions in the PPy matrix, due to their relatively large mass and site. Therefore, in agreement with similar earlier results,[36] we conclude that proton uptake is the dominant mechanism on the reduction of the films, which leads to an oxidation of the counterions (Ts^- to TsH) and simultaneous reduction of the polymer matrix (PPy^+ to PPy^0). The appearance of a gaseous species (probably H_2) at the polymer-coated electrode for high reduction potentials, forming bubbles under the PPy films, shows the permeability of the film for this species and supports the assumption of a high proton mobility in the films.

B. Analysis of the valence-band data

Now we will take a closer look at the electronic structure of the PPy films. A rough assignment of the π and σ contributions of the valence-band structures can be derived from the relative intensities at different excitation energies (Fig. 7). This classification will now be refined by comparing the measured spectra to those of the monomer[37,38] and counterions,[39,40] and to calculations of the pyrrole monomer[41] and polymer.[9,12,13,26] The calculations do not give accurate orbital energies rather than a sequence of the bands and make possible the assignment of the observed bands to the molecular orbitals of the pyrrole monomer and of the counterions. Direct comparison of the measured UPS spectra with gas-phase UPS spectra of pyrrole[37] showed an excellent agreement of the spectra (Fig. 6), underlining that the main contribution of the spectra emerges from the polymer matrix. The Ts^- ion in PPyTs does not contribute significantly to the region near the VBM in the spectra. A comparison of the XPS spectrum of TsH (Ref. 39) to our spectra in the valence-band region shows that the peak at 6.5 eV originates from the counterion and that there is some contribution to the structures at 9.4 and 25 eV from the Ts^- ion, too. The broad and relatively strong structure around 25 eV partly arises from the emission of the O 2*s* orbitals in Ts^-. The benzene ring in Ts^- should contribute to the 9.4-eV peak by the C 2*p* orbitals. The structure at 6.5 eV observed in the UPS spectra could be attributed to the strongest emission from π orbitals observed in the XPS spectra[39] and probably originates from the O 2*p* orbitals. Nevertheless, the direct comparison of XPS data with UPS data is complicated by the different photoemission cross sections. A summary of the valence-band data is given in Table I. UPS data for electrochemical prepared PPy exist up to now only for PPy films doped with ClO_4^- ions.[27] The existing differences are, of course, partly due to the different counterion used, but as the contribution of both counterions to the valence-band region is rather small, background subtraction and calibration of the spectra seem to play a more important role. The main conclusion is that the peaks in the UPS spectrum of PPyTs are mainly due to the polymer matrix.

Before discussing the UPS valence-band region near E_F in more detail, reasons should be pointed out for photoemission to be a powerful tool for investigations of the electronic structure of solids ideally suited for comparison with theoretical results. First, UPS gives a measure of the density of states of the upper orbitals in solids. For PPy, in particular, the DOS of the upper π band shows excellent agreement between theoretical investigations[9] and our measurements in the bandwidth (about 3 eV) with a high DOS at the lower band edge and a low DOS at the higher band edge. Second, the work function (Φ) and the ionization potential (I_P) can be determined by UPS. The I_P is the energy difference between the valence-band edge (E_V) and the vacuum level and is given by

$$I_P=\Phi+|E_V-E_F|=h\nu-|E_V-E_{\mathrm{SEO}}| \ . \qquad (2)$$

$h\nu$ is the excitation energy (He I) and E_{SEO} is the energy of the secondary-electron onset. UPS makes possible a separation of surface dipole and band bending or volume doping contributions, as these data are easily accessible

TABLE I. Valence-band data of pyrrole (Py) and polypyrrole (PPy). The monomer data and the calculated data are calibrated to the uppermost π orbital at 3.5 eV. The band assignment is according to that in Fig. 7.

	Energy below E_F (eV)						
UPS data	π_1	π_2		π_3,σ_1	σ_2	σ_3	σ_4
$PPClO_4$ (Ref. 27)	1.0	3.1	4.4	7.0	12.6		
PP (Ref. 23)	3.0			7.6	12.3		
PPTs (this work)	3.5	4.9	6.6	9.0	13.1		
Py (Ref. 37)	3.5	4.5		9.0	12.8		
XPS data							
PPTs (this work)				9.4	13.8	18.2	25.1
Py (Ref. 38)	3.5	4.5		9.0	13.6	18.0	24.9
Calculations							
PP (Ref. 12)	3.5	4.9		9.1	14.6	21.7	28.3
PP (Ref. 14)	3.5	5.0		8.9	15.1	22.3	30.4

from the changes in E_V and E_{SEO}. For our PPyTs films, the observed shift of E_F towards the VBM on doping is an indication of p-type conduction. For almost neutral PPy a work function of 4.2 eV is measured, giving an ionization potential of 5.4 eV.

C. Electronic excitations in PPy

Up to now only a few HREELS investigations[42] of electronic transitions in organic polymers have been known. Therefore, the interpretation of our results has to be restricted to a comparison with EELS (Ref. 18) data and optical-absorption measurements.[16,17] With respect to the energetic position and the shape of the observed structures, we find a general agreement. One advantage of EEL spectroscopy to optical-absorption measurements is the counting of single particles instead of detecting a relatively small decrease in intensity. Therefore, HREELS is a more sensitive tool in the low doping regime with small defect concentration for investigations on electronic transitions than optical-absorption spectroscopy.

The independence of vibrational transitions in the HREEL spectrum from the doping level of the samples confirms their chemical stability. The observation of combination bands and multiple vibrational energy losses is typical for organic materials. The electronic regime of the spectra, however, shows remarkable variations on doping. For a heavily reduced sample ($Y < 1\%$), there are almost no electronic transitions up to 5 eV loss energy, indicating that the reduction of the sample was almost complete. The less-reduced samples give clear evidence for polarons in the low doping regime with their observed losses at 2.0 and 2.5 eV and their characteristic relative intensities.[33] The 1.1 eV loss at intermediate doping is an electronic excitation from the half-filled polaron band into empty gap states. The slightly modulated loss continuum at high dopant concentrations results from the disappearing of the band gap during the formation of a metallic state.

The angular dependence of the loss structures in the HREEL spectra at low doping levels gives strong evidence for the existence of a dispersion relation on the PPy chain. However, the observed anisotropy in the distribution of the scattered electrons is not necessarily an indication for the existence of a macroscopic order on the surface of the PPy films. Our spectroscopic setup operates with a fixed scattering plane, which is determined by the momentum k_0 of the incident electron beam. This setup, which can be compared to an electron-diffraction experiment of randomly orientated molecules, in combination with the high anisotropy of the electronic structure of PPy, makes possible the characterization of the dispersion relation on the polymer chain even of disordered samples. In detail, electrons that have a considerable $\Delta k_{\parallel}$, compared to the width of the first Brillouin zone (0.88 Å^{-1}), are detected only if they are scattered by a polymer chain orientated almost parallel to the scattering plane. Scattering of such electrons by PPy chains having different orientations causes the electron to leave the scattering plane. Only electrons that are scattered at PPy chains orientated almost parallel to the spectroscopical plane contribute to the observed loss intensity. Therefore, we observe a make-believe order in the PPy samples. Consequently, the angular dependence of the HREEL spectra can be discussed in terms of a dispersion relation on the PPy chain. The momentum transfer along the polymer chain is related to the angle between exit angle and specular geometry θ via Eq. (1).

The strength of an electronic transition depends on the involved momentum transfer and therefore on the dispersion of the corresponding bands. Transitions between flat bands show a weak dependence of their strength on the momentum transfer, whereas transitions between bands with pronounced dispersion exhibit a strong dependence of their strength on the momentum transfer. The latter ones show a strong absorption only near the critical points at the center and the boundary of the first Brillouin zone. For other momentum transfers the absorption is weaker. The weak angular dependence in our HREEL spectra of the loss structures belonging to electronic transitions into the polaron bands indicates that these bands are rather flat. On the contrary, the uppermost π band and the lowest π^* band have to be quite broad, as the corresponding π-π^* transition shows a strong angular dependence. These findings concerning the bandwidths of the polaron, the π, and the π^* bands

are in agreement with theoretical predictions.[12,13] Our interpretation of the angular dependence of the electronic transitions is further supported by the fact that all transitions show relative maxima of the loss intensity at minima of $\Delta k_{\parallel}$ and relative minima of the loss intensity when $\Delta k_{\parallel}$ approaches half the value of the first Brillouin zone of PPy (0.44 Å^{-1}). In particular, the loss structure due to the lowest π-π^* transition disappears completely at specular geometry, because $\Delta k_{\parallel}$ matches nearly the half of the first Brillouin zone of PPy (Fig. 11). Our HREEL spectra can be compared to optical-absorption spectra only for relatively large θ (lowest spectrum in Fig. 11), when the momentum transfer is rather small. In specular geometry (uppermost spectrum in Fig. 11), our spectroscopic setup differs considerably, leading to results that are incomparable to optical data. EEL spectra[18] show a decrease of the relative intensity of the lowest π-π^* transition with increasing momentum transfer $\Delta k_{\parallel}$, too.

D. Electronic properties of intrinsic defects in PPy

Undoped PPy is an insulating material. Its band gap is determined by the Peierls instability and by symmetry reduction due to the nitrogen atom. Significant dark conductivity can only be established by doping with cations. As derived from our XPS analysis, doping with Ts^- leads to a charge transfer between the dopants and the polymer without altering the chemical structure of the polymer chains. The extra charge is stabilized as an intrinsic defect on the PPy chain. *In situ* recording of UPS and HREELS data enables us to determine the electronic properties of such intrinsic defects.

Figure 12 shows the band structure of PPy in the doping regime between 1% and 15%. At dopant concentrations below 4% our HREELS results give clear evidence for the existence of polarons. This is in agreement with

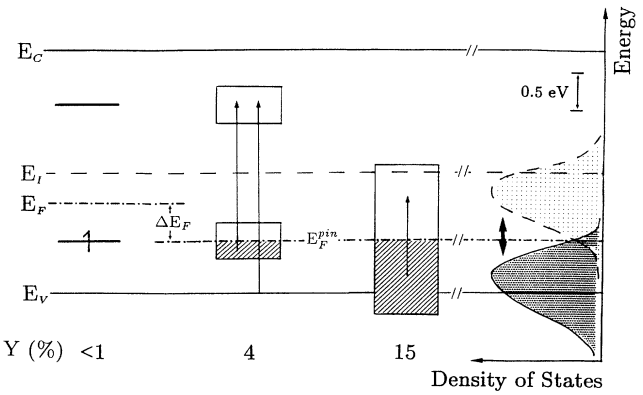

FIG. 12. Schematic energy diagram of polypyrrole at different doping concentrations Y. The diagram includes the energy levels of isolated ($Y < 1\%$) polarons and their broadening according to the spectroscopic results. The corresponding energy losses are indicated (arrows). For the metallic state ($Y \approx 15\%$), the density of states within the gap and the deconvoluted density of empty levels (dashed line) are given. The total width of the lower polaron band and the influence of repulsive electron-electron interactions (bold arrow) are indicated.

earlier data based on electrical, magnetic, and optical investigations. At intermediate doping levels ($Y \approx 15\%$) the combination of UPS and HREELS makes possible the determination of the DOS of the occupied and of the unoccupied states around E_F, as shown in the right part of Fig. 12. The occupied states are obtained from difference spectra of the valence-band data of Fig. 8. The unoccupied part is obtained by a deconvolution of the joint density of states measured in HREELS (Fig. 10) and the occupied gap states (Fig. 9) by assuming Gaussian line shapes for the involved structures. The contribution from the gap states increases continuously between 4% and 30% dopant concentration. These gap states can be assigned to interacting polarons which form bands. This is supported by our spectroscopic evidence of isolated polarons at lower dopant concentrations. At 15% doping the most interesting features of the obtained DOS are that the unoccupied gap states have almost the same width as the occupied ones and that both are located below the intrinsic Fermi level. Therefore, the observed loss structure at 1.1 eV cannot be assigned to an electronic transition from the valence band or the lower polaron band into the upper polaron band, which is expected above the intrinsic Fermi level. Rather, this loss structure must be assigned to an intraband transition within the lower polaron band. The width of the polaronic states observed in our results, even at low concentrations, appears to be larger than predicted theoretically.[10] The calculations certainly underestimate the influence of chains of different length, disorder, interchain coupling, electron-electron interactions, and interactions between chains and dopants. All of these mechanisms contribute to the width of the polaronic levels, even at low dopant concentrations.

This description of our results in terms of polarons is in line with experimental data based on electrical[11,12] and optical[16,17] measurements, as well as with recent theoretical work.[43] The appearance of occupied states in the gap and the shape of the observed DOS are inconsistent with the existence of bipolarons at elevated doping levels, because for p-like doping, bipolarons would exhibit only empty levels within the gap. Consequently, bipolarons would shift the VBM close to E_F. In contrast, we find a pinning of E_F within the gap over a wide range of doping levels. This result is somewhat contradictory to earlier investigations, especially to earlier EPR measurements, which show a decrease of the spin susceptibility per defect at about 15% doping while the conductivity further increases upon higher doping.[19] As no Pauli contribution to the spin susceptibility was observed in these EPR investigations, this behavior has been explained by the formation of bipolarons. Up to now, these results were by far the strongest arguments for favoring bipolarons to polarons at elevated doping levels. They cannot be explained by the existence of only localized polarons over a wide range of concentrations. Other independent EPR investigations do, however, report on a significant Pauli susceptibility in BF_4^--doped PPy.[44] These findings are in agreement with our results and can be explained by a decrease of the spin concentration per injected charge according to a transition from localized spins (Curie) at low

dopant concentration to delocalized spins (Pauli) in polaron bands at high dopant concentration. Another argument favoring bipolarons is a steric one: Bipolarons are able to store more charge than polarons on a polymer chain of defined length. But, assuming a defect extension of 4–7 monomeric units, as expected theoretically,[15] it is evident that strong interaction between the defects occurs at dopant concentrations, at which point these steric effects become important. In three-dimensional inorganic substances[45] similar interactions lead to a destabilization of large bipolarons. This effect is expected to be more pronounced in one-dimensional polymers like PPy because of the even stronger electron-phonon coupling.

In a recent work on polythiophene[46] (PT) UPS spectra of highly doped PT films show a DOS up to E_F, which is interpreted in terms of a polaron lattice at high dopant concentrations. Our results obtained from the similar PPy films confirm these findings. For the PT film work, however, the authors unfortunately used a preparation technique that is of limited surface cleanliness because of sample transport through air. A subsequent heat treatment most probably does not remove all adsorbed hydrocarbons from the surface. Another limitation of the preparation technique chosen there is the doping procedure, which is not electrochemically controlled. Therefore, the authors cannot present data as a function of the degree of doping.

The shape of the DOS in the gap is of particular interest in comparing our results with theoretical calculations. Before discussing this in more detail, we give a brief summary of current interpretations[47] about the shape of the DOS near E_F for organic materials as determined by UPS. Valence-band spectra of the one-dimensional metallic conductor tetrathiafulvalene-tetracyanoquinodimethane (TTF-TCNQ) salts did not show a finite DOS. Instead, a gap of about 0.3 eV was observed.[48] As an explanation, a coupling of a phonon mode to the outgoing photoelectron was suggested. The coupling strength is supposed to be enhanced by the localized wave functions of the van der Waals bonded molecules, and in a generalization is assumed to be similar for any localized system. These findings, however, are in contrast to the generally accepted metallic behavior of some of the charge-transfer salts. Metallic behavior is concluded from conductivity measurements (in bis(2,5-dimethyl-N,N′-dicyanobenzoquinonediimine) copper [(DM-DCNQI)$_2$Cu]),[49] EPR Knight shifts [in (DM-DCNQI)$_2$Cu],[50] and reflectivity measurements [in (arene)$_2X$F$_6$ (X=P,As,Sb)].[51] Metallic properties should also be reflected in the microscopic electronic structure of these compounds investigated by UPS. Due to the high surface sensitivity, the bulk electronic structure can only be derived from UPS data as long as there is no surface contamination. This explains the fact that there are only very few experimental results on the valence-band spectra of organic materials, and there are even fewer results with detailed information near E_F. As an example, for a recent study on clean surfaces, a metallic density of states has been observed in the valence-band spectra of the DCNQI salts. In particular a metallic DOS for (DM-DCNQI)$_2$Cu is observed, which is independent of temperature, and its shape of the DOS near E_F is similar to that of the Ag film used for reference.[29] The metallic state is also confirmed by temperature-dependent conductivity measurements.[29,49] Furthermore, the temperature dependence of the valence-band spectra of the Cl-substituted salts clearly indicates a metal-semiconductor transition near 100 K, in agreement with conductivity[49] and x-ray diffraction measurements.[52] Therefore, we believe that the preparation technique used in our study leads to reproducible surface structures and allows the determination of the shape of the DOS near E_F from our UPS spectra.

The observed shape of the DOS at E_F for our PPy films is not expected from the Fermi statistic of quasi-free electrons in a half-filled band, as we find a Gaussian decrease towards E_F instead of a Fermi edge. This leads us to assume that the DOS around E_F is determined by repulsive Coulomb interactions. The interactions cause a gap right at E_F. The 1.1 eV loss shown in Fig. 10 for $Y \approx 15\%$ (compare also the bold arrow to the right in Fig. 12) can be assigned to excitations from the maximum of occupied states to the maximum of empty states within the lower, half-filled polaron band in the optical gap of PPy. The occurrence of repulsive Coulomb interactions at elevated doping levels is expected from corresponding theoretical studies, which predict the importance of this type of interaction in organic polymers.[1,53]

From the theoretical point of view the influence of doping can be considered in several ways. One approach is to maintain the structure of the chain and consider the extra charge as a localized perturbation of the system. In this approach the charge is stabilized by electron-phonon coupling, or, in other words, by a partial change of the sp^2 hybridization towards a tetragonal sp^3 hybridzation. This deformation of the chain is able to host the extra electron (n-like) or the extra hole (p-like) in the created lone pair. These defects are charged by one electron (hole) and carry one spin. In most experimental studies on this type of system, p-like doping is found, i.e., an extraction of an electron from the chain.

In a recent theoretical work[43] a polaron lattice is calculated to be energetically more favorable than a bipolaron lattice (for polymers with nondegenerate ground state, such as PT) or than a soliton lattice (for polymers with a degenerate ground state, such as *trans*-polyacetylene) at high doping levels. This phenomenon results from Coulomb interactions and three-dimensional effects. The similarity of PPy and PT in their electronic and chemical properties allows us to compare our results to these calculations. Both our results and the calculations are in good agreement, as both identify polarons to be the dominant defect type on the polymer chain at high doping levels. It should be noted that only the latest theoretical works support the higher stability of polarons if compared with bipolarons. The problem in simulating the energetic behavior within a polymer is the treatment of macroscopic interaction between the chains, like disorder, crosslinking, mislinking, and the handling of correlation effects. Therefore, any calculation will be limited and reflects only an idealized case. An alternative explanation for the observed DOS in the gap can be given

in a rather different model[54] which was already discussed in the earliest approaches handling polymeric charge transport. In this approach the injected charge is not considered to be a localized perturbation but is considered to influence the ground state of the polymeric chain. In this picture, the induced charges are distributed statistically over the complete chain. With increasing concentration they tend to destabilize the degenerate ground state of the charge-density wave. Finally, this will weaken the Peierls instability and fill the gap again. As a consequence, states in the gap will appear and at finite doping concentrations a semiconductor-to-metal transition will occur. Within this disorder model, at intermediate doping concentrations electronic transitions occur that are indicative of pseudogaps in the DOS. Our observations are also consistent with predictions of this disorder model. Nevertheless, we prefer the interpretation of our results in the polaron model, as the assumption of a random distribution of the dopant molecules in the polymer matrix, as made in the disorder model for 10% doping,[54] is probably not valid for a doping level of 30%. The dopant molecules are rather expected to form a sublattice at such high dopant concentration. In addition, electrochemical investigations indicate that intercalation of the PPy films with dopant molecules increases rather than decreases the structural order of the polymer films.[55]

V. CONCLUSIONS

Significant conductivity in an idealized polymer with a linear alternating row of single and double bonds is possible only if an extra charge is introduced to the chain. The only stable way to induce charge is by implanting dopants next to the chain that enable a transfer of charge to it. Such charge transfer requires mutual interaction to the chain which may alter the structure of the chain considerably. The latter situation is realized for the ClO_4^--doped PPy films. The choice of weakly interacting counterions, on the other hand, circumvents such restrictions. This is the case for PPy films doped with the Ts^- counterion. The nonlinear variation of the N/S ratio determined by XPS upon increasing doping indicates that the doping is independent of the amount of incorporated tosylate molecules and therefore is not due to steric changes and chemical modifications. In such a system, which is close to the idealized chain, the influence of the injected charge can be studied systematically. The strong angular dependence of the loss structures at low doping levels gives clear evidence for the existence of a dispersion relation on the PPy chain and confirms the validity of discussing the electronic structure of PPy in a one-dimensional band model. For different doping levels we observe a variation of the Fermi energy as well as an increased density of states within the gap, which at high doping levels results in a finite density of states at the Fermi energy. Intragap electronic transitions are in fair agreement with calculated intragap states of polarons. The polarons are shown to interact and to form a polaron band in agreement with both the localized polaron model and the delocalized (statistical) disorder model. To explain our results, there is no need for assuming bipolaronic quasiparticles at intermediate or high doping levels.

ACKNOWLEDGMENTS

We would like to acknowledge the excellent experimental assistance of W. Neu and helpful discussions with M. Abraham and S. Roth. This work is supported by Sonderforschungsbereich 329 and Fonds der Chemischen Industrie.

[1] *Handbook of Conducting Polymers,* edited by T. A. Skotheim (Dekker, New York, 1986).

[2] H. Münstedt, *Electronic Properties of Polymers and Related Compounds,* Vol. 63 of *Springer Series in Solid-State Sciences* (Springer, Berlin, 1986), p. 8; R. S. Potember, R. C. Hoffmann, H. S. Hu, J. E. Cocchiano, C. A. Viands, R. A. Murphy, and T. O. Poehler, Polymer **28**, 574 (1987).

[3] M. A. Druy, Synth. Met. **15**, 243 (1986).

[4] D. Bloor, R. D. Hercliffe, C. G. Galiotis, and R. J. Young, *Springer Series in Solid-State Sciences,* Vol. 63 (Springer, Berlin, 1985), p. 179.

[5] B. F. Cvetko, M. P. Brungs, R. P. Barford, and M. Skyllas-Kazacos, J. Appl. Electrochem. **17**, 1198 (1987).

[6] K. K. Kanazawa, A. F. Diaz, W. D. Gill, P. M. Grant, G. B. Street, G. P. Gardini, and J. F. Kwak, Synth. Met. **1**, 329 (1979/80).

[7] A. J. Heeger, S. Kivelson, J. R. Schrieffer, and W. P. Su, Rev. Mod. Phys. **60**, 781 (1988); S. Roth and H. Bleier, Adv. Phys. **36**, 385 (1987).

[8] M. Salmon, A. F. Diaz, A. J. Logan, M. Korunbi and J. Bargon, Mol. Cryst. Liq. Cryst. **83**, 265 (1982).

[9] J. L. Brédas, B. Thémans, J. G. Fripat, J. M. André, and R. R. Chance, Phys. Rev. B **29**, 6761 (1984).

[10] J. L. Brédas, J. C. Scott, K. Yakushi, and G. B. Street, Phys. Rev. B **30**, 1023 (1984).

[11] M. Yamaura, T. Hagiwara, M. Hirasaka, T. Demura, and K. Iwata, Synth. Met. **28**, C157 (1989); M. Ogasawara, K. Funahashi, and K. Iwata, Mol. Cryst. Liq. Cryst. **118**, 159 (1985).

[12] J. M. André, D. P. Vercauteren, G. B. Street, and J. L. Brédas, J. Chem. Phys. **80**, 5643 (1984).

[13] J. L. Brédas, B. Thémans, and J. M. André, Phys. Rev. B **27**, 7827 (1983).

[14] J. L. Brédas, B. Thémans, and J. M. André, J. Chem. Phys. **78**, 6137 (1983).

[15] F. Devreux, Europhys. Lett. **1**, 233 (1986).

[16] K. Yakushi, L. J. Lauchlan, T. C. Clarke, and G. B. Street, J. Chem. Phys. **79**, 4774 (1983).

[17] P. Pfluger, M. Korunbi, G. B. Street, and G. Weiser, J. Chem. Phys. **78**, 3212 (1983).

[18] J. Fink, B. Scheerer, W. Wernet, M. Monkenbusch, G. Wegner, H. -J. Freund, and H. Gonska, Phys. Rev. B **34**, 1101 (1986).

[19] F. Genoud, M. Guglielmi, M. Nechtschein, E. Geniès, and M. Salmon, Phys. Rev. Lett. **55**, 118 (1985); F. Devreux, F. Genoud, M. Nechtschein, and B. Villeret, *Electronic Properties of Conjugated Polymers,* Vol. 76 of *Springer Series in Solid-State Sciences* (Springer, Berlin, 1987), p. 270; Synth.

Met. **18**, 89 (1987).
[20]J. H. Kaufmann, N. Colaneri, J. C. Scott, and G. B. Street, Phys. Rev. Lett. **53**, 1005 (1984); J. C. Scott, P. Pfluger, M. T. Korunbi, and G. B. Street, Phys. Rev. B **28**, 2140 (1983).
[21]S. Yueqiang, K. Carneiro, W. Ping, and Q. Renyuan, *Springer Series in Solid-State Sciences,* Vol. 76 (Springer, Berlin, 1987), p. 31; K. Bender, E. Gogu, I. Hennig, D. Schweitzer, and H. Münstedt, Synth. Met. **18**, 85 (1987); Y. Shen, K. Carneiro, C. Jacobsen, R. Qian, and J. Qiu, *ibid.* **18**, 77 (1987).
[22]S. J. Hahn, W. E. Stanchina, W. J. Gajda, and P. Vogelhut, J. Electron. Mater. **15**, 145 (1986).
[23]W. R. Salaneck, R. Erlandsson, J. Prejza, I. Lundström, and O. Inganäs, Synth. Met. **5**, 125 (1983).
[24]R. Erlandsson, O. Inganäs, I. Lundström, and W. R. Salaneck, Synth. Met. **10**, 303 (1985); T. A. Skotheim, M. I. Florit, A. Melo, and W. E. O'Grady, Phys. Rev. B **30**, 4846 (1984); J. G. Eaves, H. S. Munro, and D. Parker, Polymer Commun. **28**, 38 (1987).
[25]S. -A. Chen, Y. -C. Tsai, and S. -H. Chen, Synth. Met. **28**, C151 (1989).
[26]W. K. Ford, C. B. Duke, and W. R. Salaneck, J. Chem. Phys. **77**, 5030 (1982).
[27]P. Pfluger, U. M. Gubler, and G. B. Street, Solid State Commun. **49**, 911 (1984).
[28]A. Rager, B. Gompf, L. Dürselen, H. Mockert, D. Schmeisser, and W. Göpel, J. Mol. Electron. **5**, 227 (1989); H. Mockert, D. Schmeisser, and W. Göpel, Sensors and Actuators **19**, 159 (1989).
[29]D. Schmeisser, K. Graf, W. Göpel, J. U. von Schütz, P. Erk, and S. Hünig, Chem. Phys. Lett. **148**, 423 (1988).
[30]H. Kohler, W. Neu, K. -D. Kreuer, D. Schmeisser, and W. Göpel, Electrochim. Acta **34**, 1755 (1989).
[31]W. Wernet and G. Wegner, Makromol. Chem. **188**, 1465 (1987); D. S. Maddison, J. Unsworth, and J. Lusk, Synth. Met. **22**, 257 (1988).
[32]K. J. Wynne and G. B. Street, Macromolecules **18**, 2361 (1985); W. Wernet, M. Monkenbusch, and G. Wegner, Mol. Cryst. Liq. Cryst. **118**, 197 (1985).
[33]P. Bätz, D. Schmeisser, and W. Göpel, Solid State Commun. **74**, 461 (1990).
[34]L. F. Warren and D. P. Anderson, J. Electrochem. Soc. **134**, 101 (1987).
[35]A. F. Diaz and B. Hall, IBM J. Res. Dev. **27**, 342 (1983).
[36]T. Iyoda, A. Ohtani, T. Shimidzu, and K. Honda, Synth. Met. **18**, 725 (1987).
[37]S. Cradock, R. H. Finlay, and M. H. Palmer, Tetrahedron **29**, 2173 (1973); A. D. Baker, D. Betterridge, N. R. Kemp, and R. E. Kirby, Anal. Chem. **42**, 1064 (1970).
[38]U. Gelius, C. J. Allan, G. Johansson, H. Siegbahn, D. A. Allison, and K. Siegbahn, Phys. Scr. **3**, 237 (1971).
[39]J. Knecht and H. Bässler, Chem. Phys. **33**, 179 (1978).
[40]R. Prins and T. Novakov, Chem. Phys. Lett. **9**, 593 (1971).
[41]M. H. Palmer and A. J. Beveridge, Chem. Phys. **111**, 249 (1987); W. van Niessen, L. S. Cederbaum, and G. H. F. Dierksen, J. Am. Chem. Soc. **98**, 2066 (1976); E. Clementi, H. Clementi, and D. R. Davis, J. Chem. Phys. **46**, 4725 (1967).
[42]A. M. Botelho Do Rego, M. Rei Vilar, J. Lopes Da Silva, M. Heyman, and M. Schott, Surf. Sci. **178**, 367 (1986).
[43]S. Stafström and J. L. Brédas, Phys. Rev. B **38**, 4180 (1988); Mol. Cryst. Liq. Cryst. **160**, 405 (1988).
[44]K. Mizoguchi, M. Misoo, K. Kume, K. Kaneto, T. Shiraishi, and K. Yoshino, Synth. Met. **18**, 199 (1987).
[45]D. Emin, Phys. Rev. Lett. **62**, 1544 (1989).
[46]M. Lögdlund, R. Lazzaroni, W. R. Salaneck, S. Stafström, J. O. Nilsson, and X. Shuang, *Springer Series in Solid-State Sciences* (Springer, Berlin, in press); M. Lögdlund, R. Lazzaroni, W. R. Salaneck, and J. L. Brédas, Phys. Rev. Lett. **63**, 1841 (1989).
[47]W. D. Grobman and E. E. Koch, in *Photoemission in Solids,* edited by L. Ley and M. Cardona (Springer, Berlin, 1979), Vol. 2, p. 261.
[48]W. D. Grobman, R. A. Pollak, D. E. Eastman, E. T. Maas Jr., and B. A. Scott, Phys. Rev. Lett. **32**, 534 (1974).
[49]J. U. von Schütz, M. Bair, H. J. Gross, U. Langohr, H. -P. Werner, H. C. Wolf, D. Schmeisser, K. Graf, W. Göpel, P. Erk, H. Meixner, and S. Hünig, Synth. Met. **27**, B249 (1988).
[50]D. Köntgeter, F. Hentsch, H. Seidel, M. Mehring, P. Erk, and S. Hünig, Solid State Commun. **65**, 453 (1988).
[51]R. Wilckens, H. P. Geserich, W. Ruppel, P. Koch, D. Schweitzer, and H. J. Keller, Solid State Commun. **41**, 615 (1982); H. P. Geserich, R. Wilckens, W. Ruppel, V. Enkelmann, G. Wegner, G. Wieners, D. Schweitzer, and H. J. Keller, Mol. Cryst. Liq. Cryst. **93**, 385 (1983).
[52]A. Kobayashi, R. Kato, H. Kobayashi, T. Mori, and H. Inokuchi, Solid State Commun. **64**, 45 (1987).
[53]J. Ashkenazi, W. E. Pickett, H. Krakauer, C. S. Wang, B. M. Klein, and S. R. Chubb, Phys. Rev. Lett. **62**, 2016 (1989); F. Kajzar and J. Friedel, Phys. Rev. B **35**, 9614 (1987).
[54]E. J. Mele and M. J. Rice, Phys. Rev. B **23**, 5397 (1981).
[55]J. Heinze, R. Bilger, and K. Meerholz, Ber. Bunsenges. Phys. Chem. **92**, 1266 (1988).